

# Conformational Preferences of 1,3-Diferrocenyl-1,1,3,3-tetramethyldisiloxane and Its Cocrystal with Ferrocene: A Theoretical and Crystallographic Study of the Role of Intra- and Intermolecular Interactions

Francisco Cervantes-Lee,<sup>†</sup> Hemant K. Sharma,<sup>†</sup> Keith H. Pannell,<sup>\*,†</sup>  
 Agnes Derecskei-Kovacs,<sup>‡</sup> and Dennis S. Marynick<sup>\*,‡</sup>

Department of Chemistry and Materials Research Institute, The University of Texas at El Paso, El Paso, Texas 79968-0513, and Department of Chemistry and Biochemistry, The University of Texas at Arlington, Arlington, Texas 76019-0065

Received September 3, 1997

The solid-state structure of 1,3-diferrocenyl-1,1,3,3-tetramethyldisiloxane (**1**) exhibits significant differences between the pure crystal and the cocrystal with ferrocene. The structure of (**1**) shows that the two silicon atoms have eclipsed constituents when viewed along the Si–O–Si linkage. The structure of 1,3-diferrocenyl-1,1,3,3-tetramethyldisiloxane-ferrocene (**2**) indicates that the siloxane now exhibits a staggered conformation when viewed along the Si–O–Si linkage. To understand the origin of these differences, a nonempirical study of the energetics of very large clusters, as models of the solid state, was undertaken. PRDDO/M calculations of the relative energetics of the two different conformers of **1** show that methyl–methyl steric interactions dominate the conformational energetics and that the monomer is  $\sim 5$  kcal/mol more stable in the staggered form found in the cocrystal. However, a detailed analysis of intermolecular interactions in the pure- and cocrystals demonstrate that intermolecular interactions are more favorable in the pure crystal than in the cocrystal, resulting in the high-energy eclipsed form of the monomer being stabilized. The importance of intermolecular interactions are evaluated by calculating insertion energies of a central monomer into large clusters of molecules derived from the full lattice. The role of specific intermolecular interactions, such as ferrocene–ferrocene, ferrocene–tetramethyldisiloxane, etc., are also investigated by a similar procedure, in which either the bridge or the ferrocene components of the lattice are removed. We find that the stabilization of the eclipsed form of the monomer in the pure crystal is due dominantly to intermolecular interactions between the tetramethyldisiloxane bridges and the neighboring ferrocenes.

## Introduction

The chemistry and technology of silicon compounds has been a major stimulus for industrial and academic research laboratories since the introduction of the direct process, and in general, the study of compounds based upon silicon remains a major focus of organometallic/inorganic materials chemistry.<sup>1</sup> In addition, the incorporation of organotransition metal groups into materials chemistry has provided many exciting possibilities based upon the unusual electrical, magnetic, and optical properties of the resulting complexes and materials.<sup>2</sup> With respect to this latter aspect, the ferrocenyl (Fc) substituent,  $[(\eta^5\text{-C}_5\text{H}_5)(\eta^5\text{-C}_5\text{H}_4)\text{Fe}]$ , plays an important

role since it imparts both great thermal stability and interesting redox chemistry to the resulting systems, including siloxanes, polysilanes, and the recently reported silylene ferrocenylene polymers.<sup>3–6</sup>

An area of current interest in materials chemistry and structure/reactivity studies is the concept of crystal engineering and molecular architecture aimed at controlling the structure of solids and thin films via strategic use of synthesis.<sup>7</sup> In this paper, we report the dramatic change in conformational structure of a simple 1,3-diferrocenyl-substituted siloxane upon cocrystallization with ferrocene, i.e., FcSiMe<sub>2</sub>OSiMe<sub>2</sub>Fc (**1**) and FcSiMe<sub>2</sub>OSiMe<sub>2</sub>Fc·FcH (**2**). We have analyzed the

<sup>†</sup> The University of Texas at El Paso.

<sup>‡</sup> The University of Texas at Arlington.

(1) *Silicon Based Polymer Science: A Comprehensive Resource*; Ziegler, J. M., Fearon, F. W. G., Eds.; Advances in Chemistry Series 224, American Chemical Society: Washington, DC, 1990.

(2) (a) Zeldin, M.; Wynne, K. J.; Allock, H. R. *Inorganic and Organometallic Polymers*; ACS Symposium Series 360; American Chemical Society: Washington, DC, 1988. (b) Mark, J. E.; Allock, H. R.; West, R. *Inorganic Polymers*; Prentice Hall Polymer Science and Engineering Series; Prentice Hall: Englewood Cliffs, NJ, 1992.

(3) (a) Hayes, G. F.; George, M. H. In *Organic Polymers*; Carraher, C. E., Sheats, J. E., Pittmann, C. U., Eds.; Academic Press: New York, 1978; p 13. (b) Ozari, Y.; Sheats, J. E.; Williams, T. N.; Pittmann, C. U. *Ibid*; p 53.

(4) (a) Lin, J.; Wen, X.; Du, Z. *Shandong Daxue Zuebao, Ziran Kexueban* **1987**, *22*, 100; *Chem. Abstr.* **1988**, *109*, 74041e. (b) Du, Z.; Wen, X.; Lin, J., *Ibid*; p 115; *Chem. Abstr.* **1988**, *109*, 74041e.

(5) (a) Pannell, K. H.; Rozell, J. M.; Ziegler, J. M. *Macromolecules* **1988**, *21*, 278. (b) Pannell, K. H.; Rozell, J. M.; Vincenti, S. R. in ref 1, Chapter 20. (c) Diaz, A.; Seymour, M.; Pannell, K. H.; Rozell, J. M. *J. Electrochem. Soc.* **1990**, *137*, 503.

relative energetics of the different conformers and the contribution of various intramolecular and intermolecular interactions to these energies using the approximate ab initio molecular orbital method PRDDO/M, and we have demonstrated that the conformational energetics arise from a quite complex mixture of inter- and intramolecular effects. To our knowledge, these calculations represent the first attempt to analyze, *in a completely nonempirical fashion*, the details of inter- and intramolecular interactions in large organometallic crystals.

### Experimental Section

**Preparation of 1 and 2.** Complex **1** was synthesized by the literature procedure of Rausch and Schlemmer and recrystallized from hexane;<sup>8</sup> **2** was obtained by recrystallization of a 1:1 mixture of **1** and FcH from hexane.

**Structure Determination.** X-ray data were collected on a Nicolet/Siemens R3m/V four-circle diffractometer at room temperature, using graphite-monochromated Mo K $\alpha$  radiation and the  $\omega$  scan mode with variable speed between 3.0° and 15.0° min<sup>-1</sup> and a scan range of 1.5°. Three check reflections were monitored every hour, illustrating the stability of the crystals of **1** and **2** during the experiments.

Both structures were solved by the heavy-atom method and refined by anisotropic full-matrix least-squares minimizing  $\Sigma w(F_o - F_c)^2$ . Structure solutions and refinements were carried out with the SHELEXTL-PLUS software on a Microvax II computer. Hydrogen atoms were located at idealized positions from assumed geometries and included in least-squares and structure-factor calculations as riding atoms with isotropic thermal parameters fixed at 0.08 Å<sup>2</sup>. A semiempirical absorption correction was applied to each data set, giving min/max transmission ratios of 0.62/0.74 (**1**) and 0.89/0.68 (**2**). Crystal data and data collection parameters are provided in Table 1, and representative bond lengths and angles for **1** and **2** are presented in Table 2.

### Theoretical Calculations

The energetics of all model systems were evaluated using the method of partial retention of diatomic differential overlap (PRDDO/M),<sup>9</sup> an enhanced version of the original<sup>10</sup> PRDDO approach. PRDDO is a nonempirical molecular orbital method which has been successfully applied to many conformational

**Table 1. X-ray Crystallographic Data and Structure Refinement for 1 and 2**

compound	1	2
empirical formula	C <sub>24</sub> H <sub>30</sub> OSi <sub>2</sub> Fe <sub>2</sub>	C <sub>34</sub> H <sub>40</sub> OSi <sub>2</sub> Fe <sub>3</sub>
color; habit	orange fragment	orange fragment
cryst size (mm)	0.16 × 0.36 × 0.38	0.38 × 0.08 × 0.20
cryst syst	triclinic	triclinic
space group	<i>P</i> $\bar{1}$	<i>P</i> $\bar{1}$
unit cell dimens	<i>a</i> = 8.606(2) Å <i>b</i> = 12.568(3) Å <i>c</i> = 13.070(3) Å $\alpha$ = 61.240(15)° $\beta$ = 76.030(16)° $\gamma$ = 72.150(16)°	<i>a</i> = 7.860(2) Å <i>b</i> = 14.654(4) Å <i>c</i> = 14.721(3) Å $\alpha$ = 72.94(2)° $\beta$ = 77.01(2)° $\gamma$ = 77.01(2)°
vol	1172.2(4) Å <sup>3</sup>	1579.1(6) Å <sup>3</sup>
<i>Z</i>	2	2
2 $\theta$ range	3.5–45°	3.5–45°
scan type	$\omega$	$\omega$
scan speed	3–20°/min	3–15°/min
scan range ( $\omega$ )	1.20°	1.20°
standard rflns	3 measured every 50 reflections	3 measured every 50 reflections
index ranges	<i>h</i> : -3 to 9 <i>k</i> : -12 to 13 <i>l</i> : -13 to 14	<i>h</i> : -3 to 8 <i>k</i> : -15 to 15 <i>l</i> : -15 to 15
no. of rflns collected	3492	4393
no. of indep rflns	3046	3802
no. of obsd rflns	2745 ( <i>F</i> > 3.0 $\sigma$ ( <i>F</i> ))	3093 ( <i>F</i> > 3.0 $\sigma$ ( <i>F</i> ))
no. of abs corr	semiempirical	semiempirical
min/max transmission	0.617/0.744	0.890/0.680
final <i>R</i> indices (obsd data)	<i>R</i> = 3.08%, w <i>R</i> = 4.74%	<i>R</i> = 3.73%, w <i>R</i> = 3.20%

**Table 2. Selected Bond Lengths (Å) and Angles (deg) for 1 and 2**

	1	2
Fe1–C1	2.057(4)	2.056(4)
Fe2–C11	2.057(3)	2.056(4)
C1–Si1	1.853(4)	1.857(4)
Si1–O1	1.618(2)	1.636(3)
O1–Si2	1.627(2)	1.647(3)
Si2–C11	1.849(3)	1.849(5)
Si1–C21	1.850(4)	1.851(5)
Si2–C23	1.858(6)	1.846(4)
Fe1–C1–Si1	131.4(2)	126.3(2)
C1–Si1–O1	109.1(1)	109.1(2)
O1–Si1–C21	108.4(2)	109.9(2)
O1–Si2–C11	108.9(1)	108.5(2)
Si2–C11–Fe2	126.8(2)	127.4(2)
O1–Si2–C23	105.7(2)	108.8(2)

problems in organometallic chemistry.<sup>11</sup> It is applicable to very large systems<sup>10</sup> (the largest system studied here has over 2400 basis functions). In addition, it is expected to provide a suitable description of the intermolecular interactions in these systems, which should be dominated by dipole interactions due to the rather large number of polar bonds present. PRDDO/M employs a minimal basis set of Slater orbitals, except for transition metal d orbitals, which are described by a contracted double- $\zeta$  set of Slater functions. The method is parametrized against ab initio results (it does not contain parameters derived from experiment as is the case in semiempirical

(6) (a) Foucher, D. A.; Tang, B.-Z.; Manners, I. *J. Am. Chem. Soc.* **1992**, *114*, 6246. (b) Nguyen, M. T.; Diaz, A. F.; Dementiev, V. V.; Sharma, H.; Pannell, K. H. *SPIE Proc.* **1993**, *1910*, 230. (c) Foucher, D. A.; Ziembinski, R.; Tang, B.-Z.; Macdonald, P. M.; Massey, J.; Jaeger, C. R.; Vancso, G. J.; Manners, I. *Macromolecules* **1993**, *26*, 2878. (d) Nguyen, M. T.; Diaz, A. F.; Dementiev, V. V.; Pannell, K. H. *Chem. Mater.* **1993**, *5*, 1389. (e) Foucher, D. A.; Ziembinski, R.; Petersen, R.; Pudelski, J.; Edwards, M.; Ni, Y.; Massey, J.; Jaeger, C. R.; Vancso, G. J.; Manners, I. *Macromolecules* **1994**, *27*, 3992. (f) Dementiev, V. V.; Cervantes-Lee, F.; Párkányi, L.; Sharma, H. K.; Pannell, K. H.; Nguyen, M.-T.; Diaz, A. F. *Organometallics* **1993**, *12*, 1983. (g) Nguyen, M. T.; Diaz, A. F.; Dementiev, V. V.; Pannell, K. H. *Chem. Mater.* **1994**, *6*, 952. (h) Pannell, K. H.; Dementiev, V. V.; Li, H.; Cervantes-Lee, F.; Nguyen, M. T.; Diaz, A. F. *Organometallics* **1994**, *13*, 3644. (i) Manners, I. *Adv. Organomet. Chem.* **1995**, *37*, 131. (j) Zechel, D. I.; Hultsch, K. C.; Rulkens, R.; Balaishis, D.; Ni, Y.; Pudelski, J. K.; Lough, A. L.; Manners, I.; Foucher, D. A. *Organometallics* **1996**, *15*, 1972. (k) Ni, Y.; Rulkens, R.; Manners, I. *J. Am. Chem. Soc.* **1996**, *118*, 4102. (l) Barlow, S.; Rohl, A. L.; Shi, S.; Freeman, C. M.; O'Hare, D. *J. Am. Chem. Soc.* **1996**, *118*, 7578.

(7) *Supramolecular Architecture*; Bein, T., Eds.; ACS Symposium Series 499; American Chemical Society: Washington, DC, 1992.

(8) Rausch, M.; Schloemer, G. C. *Org. Prep. Proc.* **1969**, *1*, 131.

(9) (a) Derecskei-Kovacs, A.; Marynick, D. S. *Int. J. Quantum Chem.* **1996**, *58*, 193. (b) Derecskei-Kovacs, A.; Woon, D. E.; Marynick, D. S. *Int. J. Quantum Chem.* **1997**, *61*, 67.

(10) (a) Hålgren, T. A.; Lipscomb, W. N. *J. Chem. Phys.* **1973**, *58*, 1569. *Proc. Natl. Acad. Sci. U.S.A.* **1972**, *69*, 652. (b) Marynick, D. S.; Lipscomb, W. N. *Proc. Natl. Acad. Sci. U.S.A.* **1982**, *79*, 1341.

(11) Marynick, D. S.; Askari, S.; Nickerson, D. F. *Inorg. Chem.* **1985**, *24*, 868. Axe, F. U.; Marynick, D. S. *Organometallics* **1987**, *6*, 572. Axe, F. U.; Marynick, D. S. *J. Am. Chem. Soc.* **1988**, *110*, 3728. Hansen, L. M.; Marynick, D. S. *J. Am. Chem. Soc.* **1988**, *110*, 2358. Jolly, C. A.; Marynick, D. S. *J. Am. Chem. Soc.* **1989**, *111*, 7968. Hansen, L. M.; Marynick, D. S. *Inorg. Chem.* **1990**, *29*, 2482. Lawless, M.; Marynick, D. S. *Inorg. Chem.* **1991**, *30*, 3547. Rogers, J. R.; Kwon, O.; Marynick, D. S. *Organometallics* **1991**, *10*, 2817. Lawless, M.; Marynick, D. S. *J. Am. Chem. Soc.* **1991**, *113*, 7513. Rogers, J. R.; Marynick, D. S. *Chem. Phys. Lett.* **1993**, *205*, 197. Hansen, L. M.; Pavan Kumar, P. N. V.; Marynick, D. S. *Inorg. Chem.* **1994**, *33*, 728. Rogers, J. R.; Wagner, T. P. S.; Marynick, D. S. *Inorg. Chem.* **1994**, *33*, 3104. Rogers, J. R.; Johnson, C. K.; Marynick, D. S. *Inorg. Chem.* **1994**, *33*, 4566.

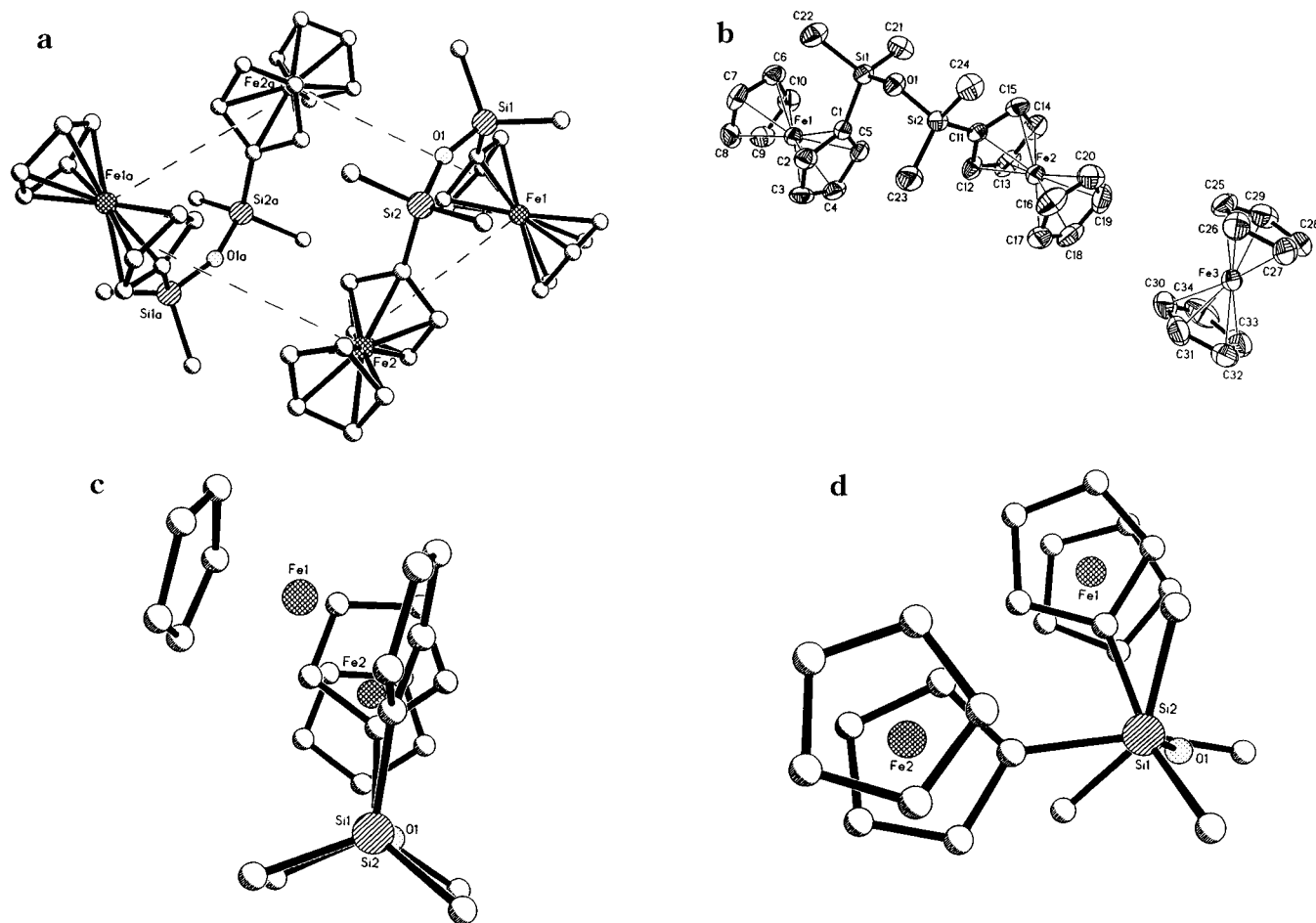


**Figure 1.** (a) Structure of 1,3-diferrocenyl-1,1,3,3-tetramethyldisiloxane (**1**). (b) Structure of 1,3-diferrocenyl-1,1,3,3-tetramethyl-disiloxane-ferrocene (**2**). (c) Projection along Si–O–Si for **1**. (d) Projection along Si–O–Si for **2**.

molecular orbital theory or molecular force fields) and may, therefore, be considered to be an approximate ab initio method.

Clusters were used to model the solid-state environment. These clusters employed the crystallographically determined geometries, except for C–H distances, which were idealized to 1.08 Å. We note that PRDDO/M yields an optimized geometry for ferrocene with an Fe–ring distance of 1.62 Å, in satisfactory agreement with the experimental value of 1.65 Å at room temperature.<sup>12</sup>

## Results and Discussion

The solid-state structure of ferrocene has been established in a series of articles<sup>12</sup> and is characterized by the well-known orthogonal orientations of neighboring ferrocenes. An overview of these packing features, discussion of similar interactions observed for bis-(benzene)chromium and nickelocene, and the factors that lead to such self-recognition and self-assembling aspects of organometallic compounds has been reported.<sup>13</sup>

The structures of **1** and **2** are presented in parts a (**1**) and b (**2**) of Figure 1 with the Newman-like projections along the Si–O–Si bonds presented for the siloxane portion of each in parts c (**1**) and d (**2**) of Figure 1. In

both complexes the various bond lengths and angles are typical of their kind. Thus, Si–C bond lengths are in the range 1.846(4)–1.858(4) Å; the C–C bond lengths are in the range 1.389(7)–1.438(6) Å; the Fe–C bond lengths are in the range of 2.030(3)–2.057(3) Å. All cyclopentadienyl rings are essentially parallel and essentially eclipsed in both molecules, and all bond angles are normal, with the only significant difference in the two molecules being that of the Si–O–Si bond, vide infra. It is immediately clear that there are significant distinctions between the siloxane portion of the two crystal structures. In **1**, the groups attached to the silicon are essentially eclipsed when viewing the projection (Si–O–Si angle = 159.9(2)°). Furthermore, the two Fc units are eclipsed and exhibit an intramolecular orthogonal relationship to each other. In **2**, the two ferrocenyl substituents on the silicon atoms are essentially parallel and the conformation about the Si–O–Si linkage (Si–O–Si angle = 141.5(1)°) exhibits the more reasonable staggered form, even though the two bulky Fc groups are not trans to each other. A ferrocenyl group of the siloxane portion interacts with a cocrystallized ferrocene unit in the orthogonal manner noted above. In both structures, the various intra- and intermolecular Fe–cyclopentadienyl centroid distances are similar, in the range 4.7–5.3 Å. These values are similar to those reported in the structure of ferrocene.<sup>12</sup> The variation of the Si–O–Si angle in the two structures suggests that the well-established flexibility of this

(12) (a) Seiler, P.; Dunitz, J. *Acta Crystallogr., Sect. B* **1979**, *35*, 2020 and references therein. (b) Calvarin, G.; Clec'h, G.; Berar, J. F.; Andre, D. *J. Phys. Chem. Solids* **1982**, *43*, 785 and references therein. (c) Seiler, P.; Dunitz, J. *Acta Crystallogr., Sect. B* **1980**, *B36*, 2255.

(13) (a) Braga, D.; Grepioni, F. *Organometallics* **1992**, *11*, 711. (b) Braga, D.; Grepioni, F. *Organometallics* **1991**, *10*, 2563.

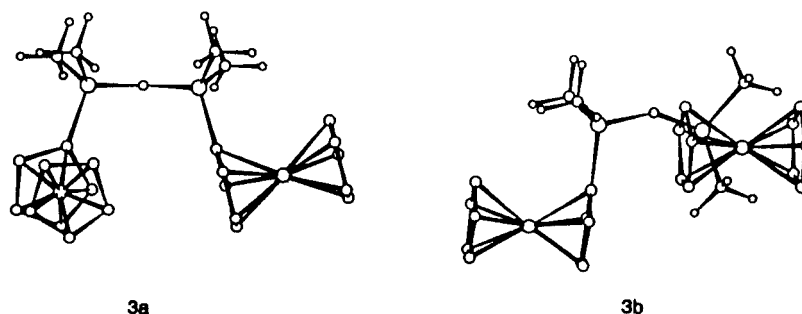


**Figure 2.** Different conformations of **1** as present in the pure crystal (**3a**) and in the cocrystal (**3b**); hydrogen atoms on the ferrocene units are omitted for clarity.

linkage (permitting a range of angles to be stable) may facilitate the observed structural variations of the molecule. A review (up to 1996) of the Cambridge Crystal Data Base records 95 structures containing the Si–O–Si linkage. The mean Si–O–Si angle is  $156.6^\circ$ , with a range from  $128.6^\circ$ <sup>14a</sup> to  $180.0^\circ$ .<sup>14b,c</sup> As noted by others, an increase in the Si–O–Si angle, i.e., from **2** ( $141.5(1)^\circ$ ) to **1** ( $159.9(2)^\circ$ ), parallels a Si–O bond length decrease: **2** (1.646(2), 1.636(2)) Å; **1** (1.618(2), 1.627(2)) Å.<sup>14d</sup>

The difference between the conformations of the siloxane portions of **1** and **2** is clearly due to some combination of intra- and intermolecular effects, and it is tempting to focus on the gross features of the nearest-neighbor interactions. In the case of **1**, together with the intramolecular Fc...Fc interaction noted above, there is a similar intermolecular interaction in the dimeric arrangement. One might think that this double Fc...Fc interaction is sufficiently strong to determine the solid-state structure of the molecule and cause the high-energy eclipsed conformation to dominate over the expected staggered form. For the cocrystal **2**, the presence of the third ferrocenyl group in the form of FcH seems to permit a packing that relieves the strain associated with the eclipsed conformation noted in **1**. A new Fc...FcH intermolecular interaction is found that results in alternating strands of FcH and FcSiMe<sub>2</sub>OSiMe<sub>2</sub>Fc with a cross-linking Fc...FcH interaction between them. However, there are many other possible intra- and intermolecular effects which could stabilize the conformation found in the pure crystal. Given the polar nature of the Fe–C and Si–O bonds, both long- and short-range Coulombic interactions could be important as well as steric effects, especially those involving the bulky tetramethyl disiloxane bridge. The qualitative effects of these Coulombic and steric interactions are, however, difficult to predict. While the relative strength of all of these interactions is unclear, knowing them is vital for the understanding of the balance between the inter- and intramolecular interactions ultimately responsible for the conformations of the molecules in the crystal.

To reveal the effects of the intra- and intermolecular interactions on the conformation of a single gas-phase molecule of 1,3-diferrocenyl-1,1,3,3-tetramethyldisiloxane (referred to from now on as the monomer), a series

**Table 3. Relative Energies of Different Conformations of **1** and Major Contributions to the Energy Difference (in kcal/mol)**

	pure crystal	cocrystal
whole monomer ( <b>3a</b> and <b>3b</b> )	0.0	–4.9
ferrocenes only ( <b>4a</b> and <b>4b</b> )	0.0	+2.2
bridge only ( <b>5a</b> and <b>5b</b> )	0.0	–6.7

of calculations at the PRDDO/M level were performed. These calculations are described in detail below.

**Conformational Energetics of the Monomer.** PRDDO/M calculations yield (Table 3) an energy difference [ $E(\mathbf{3b}) - E(\mathbf{3a})$ , see Figure 2] for the monomers of  $-4.9$  kcal/mol, favoring the conformation present in the cocrystal. This  $\Delta E$  was decomposed further by the following procedure. First, the bridging units were removed, the Fc groups were capped with hydrogens to form ferrocenes, and the energies of the two ferrocene molecules positioned in the exact locations and having the exact same orientations as in the pure crystal and in the cocrystal (structures **4a** and **4b**, respectively, in Figure 3) were calculated. This yielded a  $\Delta E$  [ $E(\mathbf{4b}) - E(\mathbf{4a})$ ] of  $+2.2$  kcal/mol, demonstrating, as expected, that the orthogonal ferrocene–ferrocene interactions found in the pure crystal are favorable. Then the relative energetics of the bridging siloxane were investigated. The Fc units were removed from the bridging groups and replaced by hydrogens, and the relative energies of the eclipsed versus staggered conformations of [SiH(CH<sub>3</sub>)<sub>2</sub>]<sub>2</sub>O (structures **5a** and **5b**, respectively, in Figure 4) were determined. The staggered bridge (**5b**) is calculated to be  $6.7$  kcal/mol more stable. The  $\Delta E$ s from the two fragment calculations sum to  $-4.5$  kcal/mol, in excellent agreement with the  $\Delta E$  obtained directly from calculations on the intact molecules. In summary, the conformational energetics of the monomer are dominated by the methyl group interactions in the bridge and the conformation found in the pure crystal is higher in energy than that of the cocrystal. Consequently, one must consider the potential stabilizing effects of intermolecular interactions to rationalize the conformation of the monomer in the pure crystal.

**Effects of Nearest Neighbors.** To estimate the relative strength of the interactions with nearest neighbors (nns) in the pure crystal and in the cocrystal, four clusters were constructed. Figure 5 illustrates clusters containing a central 1,3-diferrocenyl-1,1,3,3-tetramethyldisiloxane unit (**6a**) and a central 1,3-diferrocenyl-1,1,3,3-tetramethyldisiloxane-ferrocene unit (**6b**) and all nns molecules. Clusters **6a'** and **6b'** (not shown) are derived from **6a** and **6b** by removal of the central unit.

(14) (a) Klein, F.; Gross, J.; Witty, H.; Neagebauer, D. *Z. Naturforsch., Teil B* **1984**, *39*, 643. (b) Glidewell, C.; Liles, D. C. *J. Organomet. Chem.* **1981**, *212*, 291. (c) Auner, N.; Probst, R.; Heikenwäcker, C. R.; Herdtweck, S.; Gamper, S.; Müller, G. *Z. Naturforsch., Teil B* **1993**, *48*, 1625. (d) Baines, K. M.; Brook, A. G.; Lickess, P. D.; Sawyer, J. F. *Organometallics* **1989**, *8*, 709.

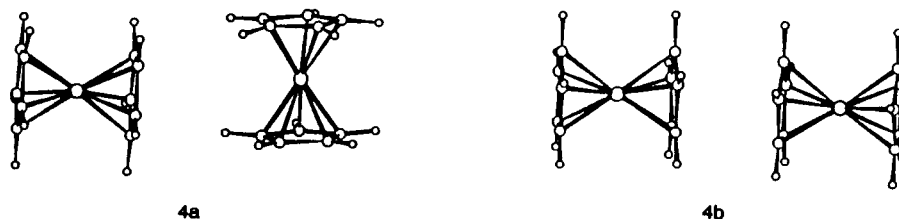


**Figure 3.** Ferrocene dimers as present in the pure crystal (**4a**) and in the cocrystal (**4b**).

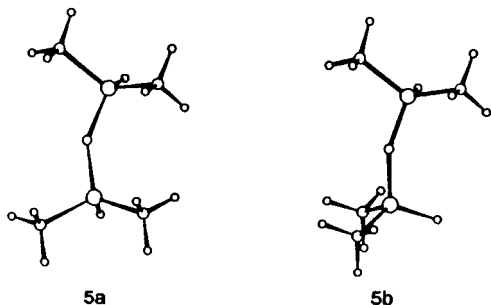


**Figure 4.** Conformers of the bridging unit with eclipsed and staggered positions of the methyl groups as present in the pure crystal (**5a**) and in the cocrystal (**5b**).

The strength of the interaction with the nns was estimated through the calculation of insertion energies  $\Delta E_i$ , calculated as follows. For the pure crystal

$$\Delta E_i(\mathbf{3a}) = E(\mathbf{6a}) - [E(\mathbf{6a}') + E(\mathbf{3a})]$$

For the cocrystal, the corresponding insertion energy is

$$\Delta E_i(\mathbf{3b}) = E(\mathbf{6b}) - [E(\mathbf{6b}') + E(\mathbf{3b})]$$

The results are summarized in Table 4.

The 5.4 kcal/mol stabilization of the monomer conformation found for the pure crystal is just enough to compensate for the isolated monomer energy difference of 4.9 kcal/mol, favoring the cocrystal conformation. However, the nature of the intermolecular interactions which are inherently responsible for this effect is still

**Table 4. Total Energies (au), Basis Set Sizes, cpu Times, and Values of Insertion Energies for Large Clusters of All Nearest Neighbors**

	pure crystal	cocrystal
$E(\mathbf{6a}$ and $\mathbf{6b})^a$	-41 794.671 56	-48 343.389 51
basis set size	2087	2435
cpu time <sup>b</sup>	169.3	297.7
$E(\mathbf{6a}'$ and $\mathbf{6b}')^a$	-37 701.294 92	-44 250.013 64
basis set size	1878	2226
cpu time <sup>b</sup>	113.8	187.6
$E(\mathbf{3a}$ and $\mathbf{3b})^a$	-4 093.318 03	-4 093.325 78
basis set size	209	209
cpu time <sup>b</sup>	0.5	0.6
insertion energies <sup>c</sup>	-36.8	-31.4

<sup>a</sup> Total energies (au). <sup>b</sup> On a NEC-SX3 computer in minutes. <sup>c</sup> kcal/mol.

unclear. Therefore, we focused on that issue in the final stages of this study.

**Fragment Analysis.** An initial attempt to model these systems with simple atom-atom pairwise potentials<sup>15</sup> proved unsuccessful. Pairwise potentials (excluding the iron atoms) predict that the insertion energy of the cocrystal is 3.2 kcal/mol *lower* than that of the monomer crystal, directly opposite to the PRDDO/M results.

To analyze the intermolecular interactions in more detail at the PRDDO/M level, two types of model lattices were created. The first type contained clusters similar to **6a** and **6b** but built *only from the Fc substituents*, with the bridges removed and Fc capped with H. The second lattice was built *only from the siloxane bridges*, with the Fc removed and the bridges capped with H. Insertion energies of similarly modified monomers were

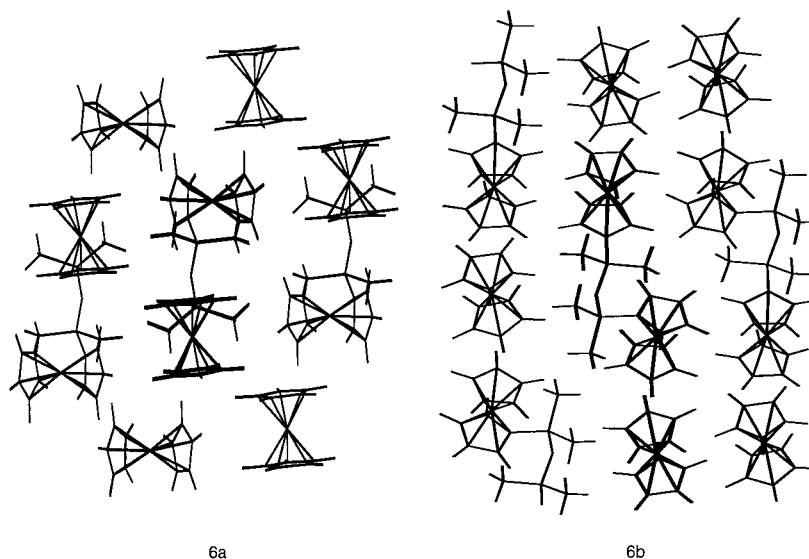


**Figure 5.** Clusters representing interactions with all the nearest neighbors in the pure crystal (**6a**) and in the cocrystal (**6b**).

then calculated. One set of monomers had only ferrocene units, while the other set had only bridges. These insertion energies were then used to characterize the intermolecular interactions between the fragments.

The results are summarized in Table 5. Our expectation was to find the major source of relative stabilization in the intermolecular ferrocene–ferrocene interactions. In fact, these interactions *destabilize* the pure crystal relative to the cocrystal by more than 4 kcal/mol. It is mainly the strong intermolecular interaction (6.8 kcal/mol) between the central ferrocene units and the bridging siloxanes of the neighboring molecules that counteracts this destabilization and ultimately yields the final relative energetics. A qualitative analysis of this ferrocene–bridge interaction energy using the repulsive part of the pairwise potentials<sup>15</sup> mentioned above suggests that steric considerations do not dominate. Indeed, the short-range repulsive interactions favor the cocrystal by nearly 5 kcal/mol. The ~7 kcal/mol stabilization calculated at the PRDDO/M level for this interaction is, therefore, due to the details of the short-range Coulombic interactions which are not modeled well by pairwise potentials (other contributions, such as dispersion energy, are not accounted for at the Hartree–Fock level and thus cannot rationalize the PRDDO/M energetics).

### Conclusion

The conformation of 1,3-diferrocenyl-1,1,3,3-tetramethyldisiloxane is strongly dependent on the crystal-

(15) Del Re, G.; Gavuzzo, E.; Giglio, E.; LeLj, F.; Mazza, F.; Zappia, V. *Acta Crystallogr.* **1977**, *B33*, 3289.

**Table 5. Relative Strength of Intermolecular Interactions between Different Segments of the Central Monomer and Different Segments of Neighboring Molecules (in kcal/mol)**

monomer segment	lattice	pure crystal	cocrystal
ferrocene	ferrocene	+4.3	0.0
bridge	bridge	+1.8	0.0
ferrocene	bridge	-6.8	0.0
bridge	ferrocene	-1.9	0.0

line environment. Nonempirical molecular orbital studies of very large molecular clusters can successfully rationalize the experimental results; however, even a qualitative understanding of the important intra- and intermolecular interactions is difficult to achieve. In particular, the conformation of this molecule is not determined by intermolecular ferrocene–ferrocene interactions but rather by interactions between the ferrocenes and the bulky tetramethyldisiloxane bridge.

**Acknowledgment.** We thank the Robert A. Welch Foundation (Grant Nos. Y-743 to D.S.M. and AH-546 to K.H.P.), the NSF (Grant No. RR-II-8802973 to K.H.P.), and the Swiss Center for High Performance Computing for support of this work.

**Supporting Information Available:** Tables of complete crystal data, data collection and refinement, atomic coordinates and equivalent isotropic displacement coefficients, complete bond lengths and angles, anisotropic displacement coefficients, and H-atom coordinates and isotropic displacement coefficients for **1** and **2** (20 pages). Ordering information is given on any current masthead page.

OM970776H